
Recurrent Parameter Generators

Jiayun Wang*¹ Yubei Chen*² Stella X. Yu¹ Brian Cheung⁴ Yann LeCun^{2,3}

¹ UC Berkeley / ICSI ² Facebook AI Research

³ New York University ⁴ MIT CSAIL & BCS

{peterwg,stellayu}@berkeley.edu

{yubeic,yann}@fb.com

cheungb@mit.edu

Abstract

We present a generic method for recurrently using the same parameters for many different convolution layers to build a deep network. Specifically, for a network, we create a recurrent parameter generator (RPG), from which the parameters of each convolution layer are generated. Though using recurrent models to build a deep convolutional neural network (CNN) is not entirely new, our method achieves significant performance gain compared to the existing works. We demonstrate how to build a *one-layer* neural network to achieve similar performance compared to other traditional CNN models on various applications and datasets. Such a method allows us to build an arbitrarily complex neural network with any amount of parameters. For example, we build a ResNet34 with model parameters reduced by more than 400 times, which still achieves 41.6% ImageNet top-1 accuracy. Furthermore, we demonstrate the RPG can be applied at different scales, such as layers, blocks, or even sub-networks. Specifically, we use the RPG to build a ResNet18 network with the number of weights equivalent to one convolutional layer of a conventional ResNet and show this model can achieve 67.2% ImageNet top-1 accuracy. The proposed method can be viewed as an inverse approach to model compression. Rather than removing the unused parameters from a large model, it aims to squeeze more information into a small number of parameters. Extensive experiment results are provided to demonstrate the power of the proposed recurrent parameter generator.

1 Introduction

Deep learning has achieved great success with increasingly more training data and deeper & larger neural networks: A recently developed NLP model, GPT-3 [1], has astonishingly 175 billion parameters! While the model performance generally scales with the number of parameters [2], with parameters outnumbering training data, the model is significantly over-parameterized. Tremendous effort has been made to reduce the parameter redundancy from different perspectives, including neural network pruning [3, 4, 5, 6], efficient network design spaces [7, 8, 9, 10], parameter regularization [11, 12, 13], model quantization [14, 15, 16], neural architecture search [17, 18, 19], recurrent models [20, 21, 22], multi-task feature encoding [23, 24], etc.

One of the most prominent approaches in this direction is the pruning-based model compression, which dates back to the late 80s or early 90s [25, 3] and has enjoyed a resurgence [4, 26] recently. These pruning methods seek to remove the unimportant parameters from a pre-trained large neural network and can frequently achieve an enormous model-compression ratio.

Though sharing a similar motivation to reduce the parameter redundancy, we explore an entirely different territory to model compression: rather than compressing a large model, we define an

*indicates equal contribution.

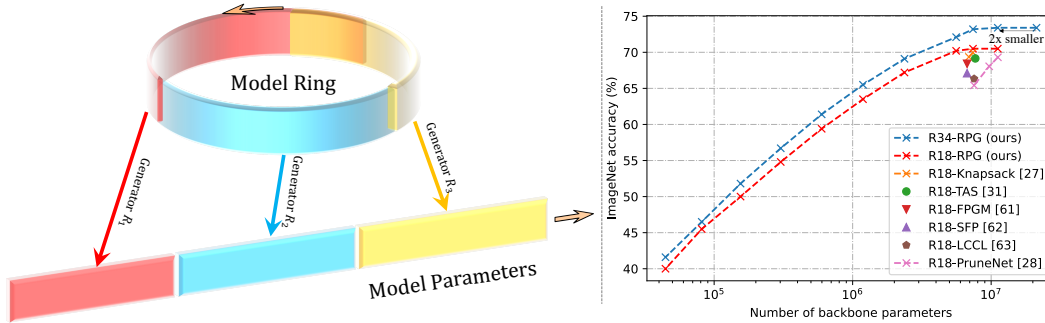


Figure 1: We propose a recurrent parameter generator (RPG) that shares a fixed set of parameters in a ring and use them to generate parameters of different parts of a neural network, whereas in the standard neural network, all the parameters are independent of each other, so the model gets bigger as it gets deeper. **Left:** The **third** section of the model starts to overlap with the **first** section in the model ring, and all later layers share generating parameters for possibly multiple times. **Right:** Employing the Recurrent Parameter Generator (RPG) for ResNet could reduce the model parameters to any size. Specifically, with only half ResNet34 backbone parameters, we achieve the same ImageNet top-1 accuracy. We also outperforms model pruning methods such as Knapsack [27] and PruneNet [28].

arbitrarily large model based on a fixed set of parameters to maximize the model capacity. In this work, we propose to define many different layers in a deep neural network based on a fixed amount of parameters, which we call *recurrent parameter generator* (RPG). We show that the excess parameter capacity can be exploited with almost no assumptions of how the parameters are assigned to the neural network architecture. In other words, there is excess capacity in neural network models independent of how and where the parameters are used in the network. Even at the level of individual scalar values, parameters can be reused in another arbitrary location of the deep network architecture without significantly impacting model performance. Surprisingly, backpropagation training of a deep network is able to cope with that the same parameter can be assigned to multiple random locations in the network without significantly impacting model performance. Through extensive experiments, we show that a large neural network does not need to be over overparameterized to achieve competitive performance. Particularly, a Resnet18 model can be implemented with the number of weights equivalent to one convolution layer in a conventional Resnet ($4.72\times$ parameter reduction) and still achieve 67.2% ImageNet top-1 accuracy. The proposed method is also extremely flexible in reducing the model parameters. In some sense, the proposed RPG method can be viewed as an automatic model pruning technique, which explores the optimal accuracy-parameter trade-off. When we reduce the model parameter, RPG shows graceful performance degradation, and its compression results are frequently on par or even better than the SOTA pruning methods besides the flexibility. Even if we reduce the Resnet18 backbone parameters to 36K, which is about $300\times$ reduction, Resnet18 can still achieve 40.0% ImageNet top-1 accuracy.

Notably, we choose a destructive parameter sharing method [29] for RPG in this work, which discourages any potential representation sharing from layer to layer. Compared to other recurrent weight-sharing methods, e.g., convolutional pose machine (CPM) or multi-scale deep equilibrium models (MDEQ), our method achieves competitive or even better performance on various benchmarks. This makes RPG a strong baseline for probing whether there is nontrivial representation sharing within any recurrent network.

To summarize, we make the following contributions:

1. We propose the recurrent parameter generator (RPG), which decouples network architecture and the number of parameters. Given a certain neural network architecture, we can flexibly choose any number of parameters to construct the network.
2. Given a compression ratio, RPG achieves on-par or even better performance compared to the state-of-the-art model pruning methods. This may provide an entirely new perspective for model compression.
3. With destructive weight sharing, RPG achieves competitive performance compared to several recurrent weight-sharing models. This makes RPG a strong baseline for probing the representation sharing for recurrent models.

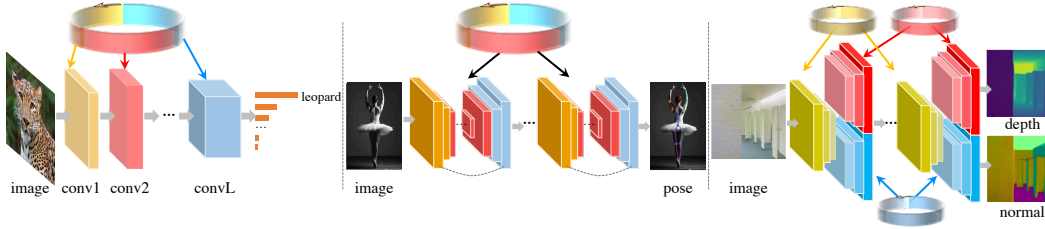


Figure 2: We demonstrate the effectiveness of RPGs on various applications including image classification (**Left**), human pose estimation (**Middle**), and multitask regression (**Right**). A network can either have a global RPG or multiple local RPGs that are shared within blocks or sub-networks.

2 Related Work

There are many important efforts to reduce the redundancy in neural network parameters. We discuss each of the approaches and their relationship to our work.

Model Pruning, Neural Architecture Search, and Quantization. As we discussed earlier, model pruning seeks to remove the unimportant parameters in a trained model. Recently, it’s proposed to use neural architecture search as a coarse-grained model pruning [30, 31]. Another related effort is neural network quantization [14, 15, 16], which seeks to reduce the bits used for each parameter and can frequently reduce the model size by $4\times$ with minimal accuracy drop. A more recent work [32] presents a framework for analyzing model scaling strategies that takes into account network properties such as FLOPs and activations.

Parameter Regularization and Priors Another highly related direction to this work is parameter regularization. Regularization has been widely used to reduce model redundancy [33], alleviate model overfitting [13, 11], and ensure desired mathematical regularity [12]. The RPG can be viewed as a parameter regularization in the sense that weight sharing poses many equality constraints to weights and regularizes weights to a low-dimensional space. HyperNeat [34] and CPPNs[35] use neural networks to determine the weight between two neurons as a function of their positions. Similarly, [36, 37] introduced a similar idea by providing a hierarchical prior for the neural network weights.

Recurrent Networks and Deep Equilibrium Models. Recurrence and feedback have been shown in psychology and neuroscience to act as modulators or competitive inhibitors to aid feature grouping [38], figure-ground segregation [39] and object recognition [40]. Recurrence-inspired mechanisms also achieve success in feed-forward models. There are two main types of employing recurrence based on if weights are shared across recurrent modules. ResNet [41], a representative of reusing similar structures without weight sharing, introduces parallel residual connections and achieves better performance by going deeper in networks. Similarly, some works [42, 43] also suggest iteratively injecting thus-far representations to the feed-forward network useful. Stacked inference methods [44, 45, 46] are also related while they consider each output in isolation. Several works find sharing weights across recurrent modules beneficial. They demonstrate applications in temporal modelling [46, 47, 48], spatial attention [49, 50], pose estimation [22, 51], and so on [52, 53]. Such methods usually shine in modeling long-term dependencies. In this work, we recurrently share weights across different layers of a feedback network to reduce network redundancy.

Given stacking weight-shared modules improve the performance, researchers consider running even infinite depth of such modules by making the sequential modules converge to a fixed point [54, 20]. Employing such *equilibrium* models to existing networks, they show improved performance in many natural language processing [20] and computer vision tasks [21, 55]. One issue with deep equilibrium models is that the forward and backward propagation usually takes much more iterations than explicit feed-forward networks. Some work [56] improves the efficiency by making the backward propagation Jacobian free. Another issue is that *infinite* depth and fixed point may not be necessary or even too strict for some tasks. Instead of achieving infinite depth, our model shares parameters to a certain level. We empirically compare with equilibrium models in Section 5.

Efficient Network Space and Matrix Factorization. Convolution is an efficient and structured matrix-vector multiplication. Arguably, the most fundamental idea in building efficient linear systems is matrix factorization. Given the redundancy in deep convolutional neural network parameters, one

can leverage the matrix factorization concept, e.g., factorized convolutions, and design more efficient network classes [7, 8, 9, 10].

3 Recurrent Parameter Generator

We define recurrent parameter generators (RPG) and show a certain kind of generating matrices that leads to destructive weight sharing. In order to achieve better parameter capacity, we introduce an even sampling strategy.

Recurrent Parameter Generator. Assuming we are constructing a deep convolutional neural network, which contains L different convolution layers. Let $\mathbf{K}_1, \mathbf{K}_2, \dots, \mathbf{K}_L$ be the corresponding L convolutional kernels². Rather than using separate sets of parameters for different convolution layers, we create a single set of parameters $\mathbf{W} \in \mathbb{R}^N$ and use it to generate the corresponding parameters for each convolution layer:

$$\mathbf{K}_i = \mathbf{R}_i \cdot \mathbf{W}, i \in \{1, \dots, L\} \quad (1)$$

where \mathbf{R}_i is a fixed predefined generating matrix, which is used to generate \mathbf{K}_i from \mathbf{W} . We call $\{\mathbf{R}_i\}$ and \mathbf{W} the *recurrent parameter generator* (RPG). In this work, we always assume that the size of \mathbf{W} is smaller than the total parameters of the model, i.e., $|\mathbf{W}| \leq \sum_i |\mathbf{K}_i|$. This means an element of \mathbf{W} will generally be used in more than one layer of a neural network. Additionally, the gradient of \mathbf{W} is a linear superposition of the gradients from each convolution layer. During the neural network training, let's assume convolution kernel \mathbf{K}_i receives gradient $\frac{\partial \ell}{\partial \mathbf{K}_i}$, where ℓ is the loss function. Based on the chain rule, it is clear that the gradient of \mathbf{W} is:

$$\frac{\partial \ell}{\partial \mathbf{W}} = \sum_{i=1}^L \mathbf{R}_i^T \cdot \frac{\partial \ell}{\partial \mathbf{K}_i} \quad (2)$$

Generating Matrices. There are many different ways to create the generating matrices $\{\mathbf{R}_i\}$. In this work, we primarily explore the destructive generating matrices, which tend to prevent different kernels from sharing the representation during weight sharing.

Destructive Weight Sharing. For easier discussion, let us first look at a special case, where all of the convolutional kernels have the same size and are used in the same shape in the corresponding convolution layers. In other words, $\{\mathbf{R}_i\}$ are square matrices, and the spatial sizes of all of the convolutional kernels have the same size, $d_{in} \times d_{out} \times w \times h$, and the input channel dimension d_{in} is always equal to the output channel dimension d_{out} . In this case, a filter \mathbf{f} in a kernel can be treated as a vector in \mathbb{R}^{dwh} . Further, we choose \mathbf{R}_i to be a block-diagonal matrix $\mathbf{R}_i = \text{block-diag}\{\mathbf{A}_i, \mathbf{A}_i, \dots, \mathbf{A}_i\}$, where $\mathbf{A}_i \in O(dwh)$ is an orthogonal matrix that rotates each filter from the kernel \mathbf{K}_i in the same fashion. Similar to the Proposition 2 in [29], we show in the Appendix B that: if $\mathbf{A}_i, \mathbf{A}_j$ are sampled from the $O(M)$ Haar distribution and $\mathbf{f}_i, \mathbf{f}_j$ are the same filter (generated by $\mathbf{R}_i, \mathbf{R}_j$ respectively from \mathbf{W}) from $\mathbf{K}_i, \mathbf{K}_j$ respectively, then we have $\mathbb{E}[\langle \mathbf{f}_i, \mathbf{f}_j \rangle] = 0$ and $\mathbb{E}\left[\left\langle \frac{\mathbf{f}_i}{\|\mathbf{f}_i\|}, \frac{\mathbf{f}_j}{\|\mathbf{f}_j\|} \right\rangle^2\right] = \frac{1}{M}$. Since M is usually large, the same filter from $\mathbf{K}_i, \mathbf{K}_j$ are close to orthogonal and generally dissimilar. This shows that even $\{\mathbf{K}_i\}$ are generated from the same \mathbf{W} , they are not sharing the representation.

Even though $\{\mathbf{A}_i\}$ are not updated during the training, the size of \mathbf{A}_i can be quite large in general. In practice, we can use permutation $p \in P(M)$ and element-wise random sign reflection $b \in B(M)$ to construct a subset of the orthogonal group $O(M)$, i.e. we choose $\mathbf{A}_i \in \{b \circ p \mid b \in B(M), p \in P(M)\}$.³ Since pseudo-random numbers are used, it takes only two random seeds to store a random permutation and an element-wise random sign reflection.

In this work, we generalize the usage of \mathbf{R}_i beyond the block-diagonal generating matrices described above. $\{\mathbf{K}_i\}$ may have different sizes, which can be chosen even larger than the size of \mathbf{W} . When $\mathbf{K}_i \in \mathbb{R}^{N_i}$ is larger than $\mathbf{W} \in \mathbb{R}^N$, the corresponding generating matrix \mathbf{R}_i is a tall matrix.

²In this paper, we treat each convolutional kernel as a vector. When the kernel is used to do the convolution, it will be reshaped into the corresponding shape.

³Permutations and element-wise random sign reflection conceptually are subgroups from the orthogonal group, but we shall never use them in the matrix form for the obvious efficiency purpose.

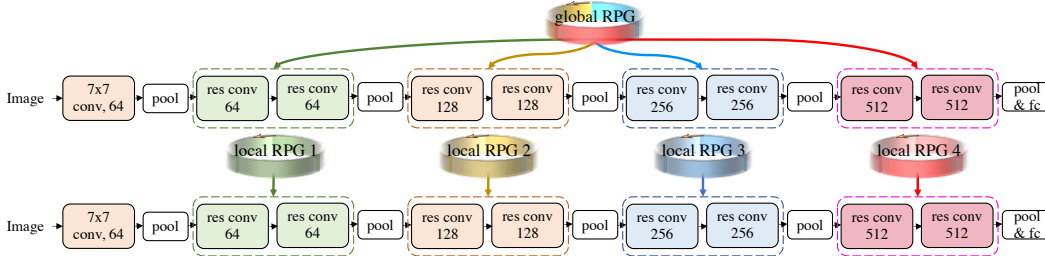


Figure 3: Recurrent parameter generators at multiple scales. **Upper:** A global RPG is used for generating convolution kernels for the entire ResNet18. **Lower :** Four local RPGs are each responsible for generating convolution kernels within each corresponding building block of the ResNet18.

There are many ways to efficiently create the generating matrices. We use random permutations $P(N_i)$ and element-wise random sign reflections $B(N_i)$ to create R_i :

$$R_i \in \{b \circ p \mid b \in B(N_i), p \in P(N_i)\}, i = 1, \dots, L \quad (3)$$

$\{R_i\}$ tend to lead to destructive weight sharing and lead to better utilization of the parameter capacity.

Even Parameter Distribution for Different Layers. While it is easy to randomly sample elements from the \mathbf{W} when generating parameters for each layer, it may not be optimal as some elements in \mathbf{W} may never be used, and some elements may be used more than average. We use an equalization technique to guarantee all elements of \mathbf{W} are evenly sampled. Suppose the size of the \mathbf{W} is N , and the total size of parameters of layers to be generated is M , $M > N$. We first generate $\lfloor \frac{M}{N} \rfloor$ arrays $\{x \mid x = 1, \dots, N\}$ and concatenate them with $(M \bmod N)$ elements randomly sampled from array $\{x \mid x = 1, \dots, M\}$. We call the concatenated array index array $u \in \mathbb{R}^M$. We randomly shuffle all elements in u . When initializing each layer’s parameter, we sequentially get indices of chosen elements from the shuffled index array u . In this way, each layer’s parameters are randomly and evenly sampled from \mathbf{W} . We refer to \mathbf{W} as *model rings* since elements are recurrently used in a loop. For data saving efficiency, we just need to save two random seed numbers (one for sampling $(M \bmod N)$ elements and one for shuffling) instead of saving the large index array u .

Batch Normalization. We find the model performance is relatively sensitive to the batch normalization parameters. To achieve better performance, each of the convolution layers needs to have its own batch normalization parameters. But in general, batch normalization is relatively negligible. We show later that when \mathbf{W} is extremely small (e.g., 36K parameters), the size of batch normalization should be considered.

4 Recurrent Parameter Generator at Multiple Scales

In the previous section, we discuss the general idea of superposition where only one RPG is created and shared globally across all layers. We could also create several local RPGs, and each of them is shared at certain scales, such as blocks and sub-networks. Such super-positions may be useful for certain applications such as recurrent modeling.

RPGs at Block-Level. Researchers propose network architectures that reuse the same design of network blocks multiple times for higher learning capacity, as discussed in the related work. Instead of using one global RPG for the entire network, we could alternatively create several RPGs that are shared within certain network blocks. We take ResNet18 [41] as a concrete example (Fig.3). ResNet18 has four building blocks. Every block has 2 residual convolution modules. To superpose ResNet18 at block scale, we create four local RPGs. Each RPG is shared within the corresponding building block, where the size of the RPG is flexible and can be determined by users.

RPGs at Sub-Network-Level. Reusing sub-networks, or recurrent networks have achieved success in many tasks as they iteratively refine and improves the prediction. Usually, weights are shared when reusing the sub-networks. This may not be optimal as sub-networks at different stages iteratively improve the prediction, and shared weights may limit the learning capacity to adapt for different

stages. On the other hand, not sharing weights at all greatly increases the model size. We superpose different sub-networks with one or more RPGs. Superposition sub-networks could have a much smaller model size, while parameters for different sub-networks undergo destructive changes instead of directly copy-paste. We show applications of superpose sub-networks for pose estimation and multitask regression (Section 5.3 and 5.4).

5 Experimental Results

We conduct 3 sets of experiments to evaluate the proposed superposition method (with tasks illustrated in Fig.2). The first set benchmarks the performance of RPG networks on image classification datasets including CIFAR100 and ImageNet. We compare with deep equilibrium models, a strong baseline on exploiting model capacity with limited model size. The second set benchmarks the performance of RPG at block and sub-network level on human pose estimation and multi-task regression datasets. We compare with recurrent models as baselines. The last set provide additional analysis and ablation studies of RPG networks Experiments are conducted on NVIDIA GeForce GTX 2080Ti GPUs.

5.1 CIFAR Classification

We benchmark the performance of the proposed RPG network on CIFAR10 and CIFAR100 datasets.

Implementation Details. All CIFAR experiments use batchsize of 128, weight decay of $5e-4$, and initial learning rate of 0.1 with gamma of 0.1 at epoch 60, 120 and 160.

Compared to Deep Equilibrium Models. As a representative of implicit models, deep equilibrium models [20] can reduce model redundancy by finding fix points via additional optimizations. We compare the image classification accuracy on CIFAR10 and CIFAR100 datasets, as well as the inference time on CIFAR100 (Table 1). Following the settings of MDEQ [21], an image was sequentially fed into the initial convolutional block, the multi-scale deep equilibrium block (dubbed as *MS* block), and the classification head. MDEQ [21] achieves *infinite* MS blocks by finding the fixed point of the MS block. We reuse the MS block two to four times without increasing the number of parameters. Our superposition method achieves 3.4% - 5.8% gain on CIFAR10 and 3% - 5.9% gain on CIFAR100. Our inference time is 15 - 25 times smaller than MDEQ since MDEQ needs additional time to solve equilibrium during training.

Global RPG with Varying # Parameters. We create one global RPG to generate parameters for convolution layers of ResNet [41] and refer to it as *ResNet-RPG*. We report CIFAR100 top-1 accuracy of ResNet-RPG18 and ResNet-RPG34 at different number of parameters (Fig.4 and Table 3). Compared to ResNet, ResNet-RPG achieves higher accuracy at the same parameter size. Specifically, we achieve 36% CIFAR100 accuracy with only 8K backbone parameters. Furthermore, ResNet34-RPG achieves higher accuracy than ResNet18-RPG, indicating increasing time complexity gives performance gain.

Local RPGs at the Block-Level. In the previous ResNet-RPG experiments, we use one global RPG (Fig.3-Upper). We also evaluate the performance when RPGs are shared locally at a block level, as shown in Fig.3-Lower. In Table 2, compared to plain ResNet18 at the same number of parameters, our block superposition network gives 1.0% gain. In contrast, our ResNet-RPG (parameters are evenly distributed) gives a 1.4% gain. Using one global RPG where parameters of each layer are evenly distributed is 0.4% higher than multiple RPGs.

Table 1: Our method compared with multiscale deep equilibrium models [21] on CIFAR10 and CIFAR100 classification. At the same number of model parameters, we achieve 3% - 6% improvement with 15 - 25x less inference time. Inference time is measured by milliseconds per image.

	MDEQ [21]	Our RPG		
		2x MS blk	3x MS blk	4x MS blk
CIFAR10 acc. (%)	85.1	88.5	90.1	90.9
CIFAR100 acc. (%)	59.8	62.8	64.7	65.7
Inference time	3.15	0.12	0.18	0.22

Table 2: At the same number of backbone parameters on CIFAR100, using local RPGs at block-level improves accuracy. Using a global RPG further improves the accuracy.

	#Param	Acc. (%)
Res18	11M	77.5
Res34-RPG.blk	11M	78.5
Res34-RPG	11M	78.9
Res34	21M	79.1

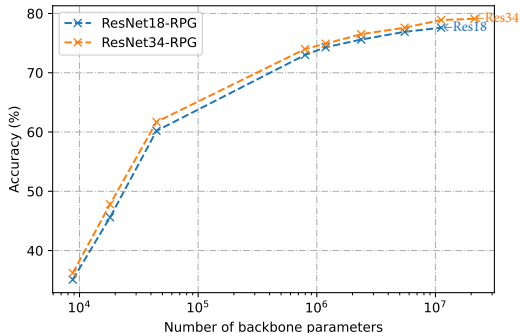


Figure 4: CIFAR100 accuracy versus the number of backbone parameters for plain ResNet and ours. We only have a 0.2% drop with 50% Res34 backbone parameters.

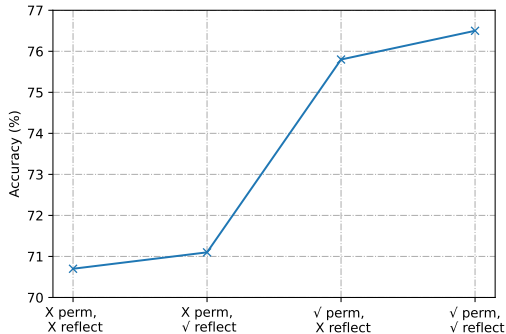


Figure 5: Ablation studies of permutation and reflection matrices. Having both matrices gives the highest performance.

Table 3: ImageNet and CIFAR100 top-1 classification accuracy versus the number of backbone parameters for our ResNet-RPG and plain ResNet. Our ResNet-RPG consistently achieves higher performance at the same number of parameters.

	ResNet18	ResNet34	Our Res18-RPG	Our Res34-RPG
# Parameters	11M	21M	45K 2M	45K 2M 11M
ImageNet Acc. (%)	69.8	73.4	40.0 67.2	41.6 69.1 73.4
CIFAR100 Acc. (%)	77.6	79.1	60.2 75.6	61.7 76.5 78.9

5.2 ImageNet Classification

Implementation Details. All ImageNet experiments use batch size of 256, weight decay of $3e-5$, and an initial learning rate of 0.3 with gamma of 0.1 every 75 epochs.

Superposition with Varying # Parameters. We use one RPG with different number of parameters for ResNet and report the top-1 accuracy (Table 3 and Fig.1(Right)). ResNet-RPGs consistently achieve higher performance compared to ResNets under the same number of parameters. Specifically, ResNet-RPG34 achieves the same accuracy 73.4% as ResNet34 with only half of ResNet34 backbone parameters. ResNet-RPG18 also achieves the same accuracy as ResNet18 with only half of ResNet18 backbone parameters. Further, we find RPG networks have higher generalizability (Section 5.5).

Power Law. Empirically, accuracy and number of parameters follow a power law, when RPG model size is lower than 50% original plain ResNet model size. The exponents of the power laws are the same for ResNet18-RPG and ResNet34-RPG on ImageNet, when comparing with ResNet34 accuracies. The scaling law may be useful for estimating the network performance without training the network. Similarly, [2] also identifies a power law for performance and model size of transformers. The proposed RPG enables *under-parameterized* models for large-scale datasets such as ImageNet, which may unleash more new studies and findings.

5.3 Pose Estimation

Implementation Details. We superpose sub-networks for pose estimation with a globally shared RPG (Fig.6). We use hourglass networks [59] as the building backbone. The input image is first fed

Table 4: Pose estimation performance (number of parameters) on MPII human pose dataset [57]. The metric is PCKh@0.5.

	CPM [22]	Ours	No shared w.
1x sub-net		84.7 (3.3M)	
2x sub-nets	86.1 (3.3M)	86.5 (3.3M)	87.1 (6.7M)
4x sub-nets	86.5 (3.3M)	87.3 (3.3M)	88.0 (13.3M)

Table 5: Multitask regression errors on S3DIS [58]. Lower is better. Number of parameters for different methods are the same.

	Depth RMSE	Normal RMSE
No reusing the sub-net [23]	25.5%	41.0%
Reuse sub-net	24.7%	40.3%
Reuse & new BN	24.0%	39.4%
Reuse & new BN & perm. and reflect.	22.8%	39.1%

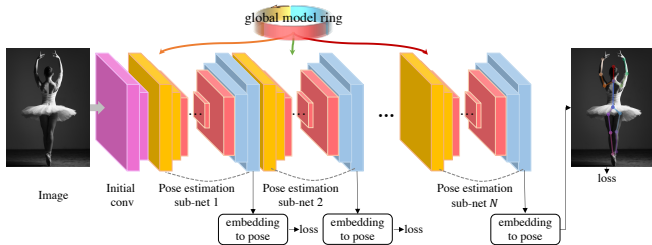


Figure 6: Pose estimation with sub-network superposition. An input image is fed to an initial convolutional block and N stacked pose estimation networks. Each sub-network predicts the pose that are penalized by corresponding loss. Parameters of each sub-network are generated from a global RPG.

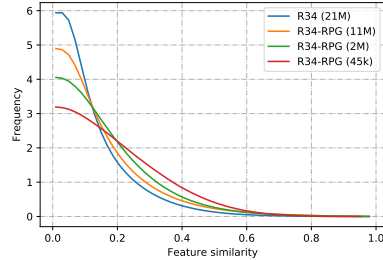


Figure 7: Normalized histogram of feature similarity for Res34-RPG with different model parameters. Feature similarity increases as the model size decreases, indicating our RPG networks can be further pruned with methods like [60].

to an initial convolution block to obtain a feature map. The feature map is then fed to multiple stacked pose estimation sub-networks. Each sub-network outputs a pose estimation prediction, which is penalized by the pose estimation loss. Convolutional pose machine (CPM) [22] share all the weights for different sub-networks. We create one global RPG and generate parameters for each sub-network. Our model size is set to be the same as CPM. We also compare with larger models where parameters of sub-networks are not shared.

We evaluate on MPII Human Pose dataset [57], a benchmark for evaluation of articulated human pose estimation, which consists of more than 28K training samples over 40K people with annotated body joints. We use the hourglass network as backbone [59] and follow all their settings.

Results and Analysis. We report the Percentage of Correct Key-points at 50% threshold (PCK@0.5) of different methods in Table 4. CPM [22] share all parameters for different sub-networks. We use one RPG that is shared globally at the same size as CPM. For reference, we also compare with the no-sharing model as the performance ceiling. Adding the number of recurrences leads to performance gain for all methods. At the same model size, our superposition models achieve higher PCK@0.5 compared to CPM. Increasing the number of parameters by not sharing sub-network parameters also leads to some performance gain.

5.4 Multi-Task Regression

Implementation Details. We superpose sub-networks for multi-task regression with multiple RPGs at the building-block level. We focus on predicting depth and normal maps from a given image. We stack multiple SharpNet [23], a network for monocular depth and normal estimation. Specifically, we create multiple RPGs at the SharpNet building-block level. In other words, parameters of corresponding blocks of different sub-networks are generated from the same RPG.

We evaluate the monocular depth and normal prediction performance on Stanford 3D indoor scene dataset [58]. It contains over 70K images with corresponding depths and normals covering over 6,000 m² indoor area. We follow all settings of SharpNet [23], a state-of-the-art monocular depth and normal estimation network.

Results and Analysis. We report the mean square errors for depth and normal estimation in Table 5. Compared to one-time inference without recurrence, our RPG network gives 3% and 2% gain for depth and normal estimation, respectively. Directly sharing weights but using new batch normalization layers decrease the performance by 1.2% and 0.3% for depth and normal. Sharing weights and normalization layers further decrease the performance by 0.7% and 0.9% for depth and normal.

5.5 Analysis

Comparison to Pruning Methods. We report our ResNet18-RPG performance with different number of parameters on ImageNet and some baseline pruning methods in Fig.1 (Right). Our RPG networks outperform SOTA pruning methods such as [27, 31, 62, 63, 64, 28]. Specifically, at the

Table 6: The proposed RPG increases the model generalizability. **(a)** ResNet with RPG has the lower gap between training and validation set on ImageNet classification. The metric is training accuracy minus validation accuracy. Lower is better. **(b)** Using RPG for pose estimation also decreases the training and validation performance GAP. The metric is training PCK@0.5 minus validation PCK@0.5. Lower is better. **(c)** ResNet with RPG has higher performance on out-of-distribution dataset ObjectNet [61]. The model is trained on ImageNet only and directly evaluated on ObjectNet.

(a)			(b)				(c)			
	ResNet	ours		no shared w	shared w [22]	ours		R18	R34-RPG	R34
18 conv	-0.7	-2.7	2x sub-nets	1.15	1.13	0.64	# Params	11M	11M	21M
34 conv	1.1	-2.3	4x sub-nets	1.98	1.70	1.15	Acc. (%)	13.4	16.5	16.0

same number of parameters, our RPG network has 0.6% gain over the knapsack pruning [27], a method that achieves the best ImageNet pruning accuracy.

Generalizability. To understand generalizability of proposed RPG networks, we report the performance gap between training and validation set on ImageNet (Table 6(a)) and MPII pose estimation (Table 6(b)). Superposition models consistently achieve lower gaps between training and validation set, indicating the superposition model suffers less from over-fitting.

We also report the out-of-distribution performance of superposition models. ObjectNet [61] contain 50k images with 113 classes overlapping with ImageNet. Previous models are reported to have a large performance drop on ObjectNet. We directly evaluate the performance of ImageNet-trained model on ObjectNet without any fine-tuning (Table 6(c)). With the same number of backbone parameters, our ResNet-RPG achieves a 3.1% gain compared to ResNet18. With the same network architecture design, our ResNet-RPG achieves 0.5% gain compared to ResNet34. This indicates our RPG networks have higher out-of-distribution performance even with smaller model sizes.

Feature Similarity. RPG networks are small in parameter size, are they still possible to prune? Some work [60] achieves satisfactory pruning results by calculating the correlation matrix of a feature map from the network, and prune channels with high correlations. Following their settings, we report feature similarity of ResNet34-RPG after residual building block 3 (Fig.7). From our small ResNet34-RPG with 45k backbone parameters to plain ResNet34 with 21M backbone parameters, the feature similarity gradually increases. This indicates our RPG networks can still be pruned, and the FLOPs and run time can be further reduced. We provide empirical pruning results in Appendix A.

Security. Permutation matrices generated by the random seed can be considered as security keys to decode the model. In addition, only random seeds to generate transformation matrices need to be saved and transferred, which is efficient in terms of size.

5.6 Ablation Studies

We conduct ablation studies to understand the functions of permutation and reflection matrices (Fig.5). We evaluate ResNet-RPG34 with 2M backbone parameters. With permutation and reflection matrices leads to 76.5% accuracy, with permutation matrices only leads to 75.8%, with reflection matrices only leads to 71.1%, and with no permutation and reflection matrices leads to 70.7%. This suggests permutation and reflection matrices are useful for RPGs.

6 Discussion

In this work, we limit our scope to linear destructive weight sharing for different convolutional layers. However, in general, there might also exist nonlinear RPGs and efficient nonlinear generation functions to create convolutional kernels from a shared parameter \mathbf{W} . Additionally, although we focus on reducing model parameters, results in Fig.7 indicate RPG networks are compressible, and it is possible to further reduce the FLOPs and run time.

To sum up, we develop an efficient approach to build an arbitrarily complex neural network with any amount of parameters via a recurrent parameter generator. On a wide range of applications, including image classification, pose estimation and multitask regression, we show RPG networks consistently

achieve higher performance at the same model size. Further, analysis shows that such networks are less possible to overfit and have higher performance on out-of-distribution data.

RPG can be added to any existing network flexibly with any amount of total parameters at the user’s discretion. It may provide new perspectives for recurrent models, equilibrium models, and model compression.

References

- [1] Tom B Brown, Benjamin Mann, Nick Ryder, Melanie Subbiah, Jared Kaplan, Prafulla Dhariwal, Arvind Neelakantan, Pranav Shyam, Girish Sastry, Amanda Askell, et al. Language models are few-shot learners. In H. Larochelle, M. Ranzato, R. Hadsell, M. F. Balcan, and H. Lin, editors, *Advances in Neural Information Processing Systems*, volume 33, pages 1877–1901. Curran Associates, Inc., 2020.
- [2] Tom Henighan, Jared Kaplan, Mor Katz, Mark Chen, Christopher Hesse, Jacob Jackson, Heewoo Jun, Tom B Brown, Prafulla Dhariwal, Scott Gray, et al. Scaling laws for autoregressive generative modeling. *arXiv preprint arXiv:2010.14701*, 2020.
- [3] Yann LeCun, John S Denker, and Sara A Solla. Optimal brain damage. In *Advances in neural information processing systems*, pages 598–605, 1990.
- [4] Song Han, Huizi Mao, and William J Dally. Deep compression: Compressing deep neural networks with pruning, trained quantization and Huffman coding. In *Proceedings of the International Conference on Learning Representations*, 2016.
- [5] Zhuang Liu, Mingjie Sun, Tinghui Zhou, Gao Huang, and Trevor Darrell. Rethinking the value of network pruning. In *International Conference on Learning Representations*, 2018.
- [6] Jonathan Frankle and Michael Carbin. The lottery ticket hypothesis: Finding sparse, trainable neural networks. In *International Conference on Learning Representations*, 2018.
- [7] Andrew G Howard, Menglong Zhu, Bo Chen, Dmitry Kalenichenko, Weijun Wang, Tobias Weyand, Marco Andreetto, and Hartwig Adam. Mobilenets: Efficient convolutional neural networks for mobile vision applications. *arXiv preprint arXiv:1704.04861*, 2017.
- [8] Forrest N Iandola, Song Han, Matthew W Moskewicz, Khalid Ashraf, William J Dally, and Kurt Keutzer. Squeezenet: Alexnet-level accuracy with 50x fewer parameters and < 0.5 mb model size. *arXiv preprint arXiv:1602.07360*, 2016.
- [9] Mingxing Tan and Quoc Le. Efficientnet: Rethinking model scaling for convolutional neural networks. In *International Conference on Machine Learning*, pages 6105–6114, 2019.
- [10] Mark Sandler, Andrew Howard, Menglong Zhu, Andrey Zhmoginov, and Liang-Chieh Chen. Mobilenetv2: Inverted residuals and linear bottlenecks. In *Proceedings of the IEEE conference on computer vision and pattern recognition*, pages 4510–4520, 2018.
- [11] Li Wan, Matthew Zeiler, Sixin Zhang, Yann Le Cun, and Rob Fergus. Regularization of neural networks using dropconnect. In *International conference on machine learning*, pages 1058–1066. PMLR, 2013.
- [12] Jiayun Wang, Yubei Chen, Rudrasis Chakraborty, and Stella X Yu. Orthogonal convolutional neural networks. In *Proceedings of the IEEE/CVF Conference on Computer Vision and Pattern Recognition*, pages 11505–11515, 2020.
- [13] Nitish Srivastava, Geoffrey Hinton, Alex Krizhevsky, Ilya Sutskever, and Ruslan Salakhutdinov. Dropout: a simple way to prevent neural networks from overfitting. *The journal of machine learning research*, 15(1):1929–1958, 2014.
- [14] Itay Hubara, Matthieu Courbariaux, Daniel Soudry, Ran El-Yaniv, and Yoshua Bengio. Quantized neural networks: Training neural networks with low precision weights and activations. *The Journal of Machine Learning Research*, 18(1):6869–6898, 2017.
- [15] Mohammad Rastegari, Vicente Ordonez, Joseph Redmon, and Ali Farhadi. Xnor-net: Imagenet classification using binary convolutional neural networks. In *European conference on computer vision*, pages 525–542. Springer, 2016.
- [16] C Louizos, M Reisser, T Blankevoort, E Gavves, and M Welling. Relaxed quantization for discretized neural networks. In *International Conference on Learning Representations*. International Conference on Learning Representations, ICLR, 2019.

- [17] Barret Zoph and Quoc V Le. Neural architecture search with reinforcement learning. *arXiv preprint arXiv:1611.01578*, 2016.
- [18] Han Cai, Ligeng Zhu, and Song Han. Proxylessnas: Direct neural architecture search on target task and hardware. In *International Conference on Learning Representations*, 2018.
- [19] Alvin Wan, Xiaoliang Dai, Peizhao Zhang, Zijian He, Yuandong Tian, Saining Xie, Bichen Wu, Matthew Yu, Tao Xu, Kan Chen, et al. Fbnetv2: Differentiable neural architecture search for spatial and channel dimensions. In *Proceedings of the IEEE/CVF Conference on Computer Vision and Pattern Recognition*, pages 12965–12974, 2020.
- [20] Shaojie Bai, J Zico Kolter, and Vladlen Koltun. Deep equilibrium models. *Advances in Neural Information Processing Systems*, 32:690–701, 2019.
- [21] Shaojie Bai, Vladlen Koltun, and J Zico Kolter. Multiscale deep equilibrium models. *Advances in Neural Information Processing Systems*, 33, 2020.
- [22] Shih-En Wei, Varun Ramakrishna, Takeo Kanade, and Yaser Sheikh. Convolutional pose machines. In *Proceedings of the IEEE conference on Computer Vision and Pattern Recognition*, pages 4724–4732, 2016.
- [23] Michael Ramamonjisoa and Vincent Lepetit. Sharpnet: Fast and accurate recovery of occluding contours in monocular depth estimation. *The IEEE International Conference on Computer Vision (ICCV) Workshops*, 2019.
- [24] Yongchang Hao, Shilin He, Wenxiang Jiao, Zhaopeng Tu, Michael Lyu, and Xing Wang. Multi-task learning with shared encoder for non-autoregressive machine translation. *arXiv preprint arXiv:2010.12868*, 2020.
- [25] Michael C Mozer and Paul Smolensky. Using relevance to reduce network size automatically. *Connection Science*, 1(1):3–16, 1989.
- [26] Davis Blalock, Jose Javier Gonzalez Ortiz, Jonathan Frankle, and John Guttag. What is the state of neural network pruning? *arXiv preprint arXiv:2003.03033*, 2020.
- [27] Yonathan Aflalo, Asaf Noy, Ming Lin, Itamar Friedman, and Lihi Zelnik. Knapsack pruning with inner distillation. *arXiv preprint arXiv:2002.08258*, 2020.
- [28] Ashish Khetan and Zohar Karnin. Prunenet: Channel pruning via global importance. *arXiv preprint arXiv:2005.11282*, 2020.
- [29] Brian Cheung, Alex Terekhov, Yubei Chen, Pulkit Agrawal, and Bruno Olshausen. Superposition of many models into one. In *Advances in neural information processing systems*, 2019.
- [30] Jiahui Yu, Linjie Yang, Ning Xu, Jianchao Yang, and Thomas Huang. Slimmable neural networks. *arXiv preprint arXiv:1812.08928*, 2018.
- [31] Xuanyi Dong and Yi Yang. Network pruning via transformable architecture search. In H. Wallach, H. Larochelle, A. Beygelzimer, F. d’Alché-Buc, E. Fox, and R. Garnett, editors, *Advances in Neural Information Processing Systems*, volume 32. Curran Associates, Inc., 2019.
- [32] Piotr Dollár, Mannat Singh, and Ross Girshick. Fast and accurate model scaling. In *Proceedings of the IEEE/CVF Conference on Computer Vision and Pattern Recognition*, pages 924–932, 2021.
- [33] Anders Krogh and John A Hertz. A simple weight decay can improve generalization. In *Advances in neural information processing systems*, pages 950–957, 1992.
- [34] Kenneth O Stanley, David B D’Ambrosio, and Jason Gauci. A hypercube-based encoding for evolving large-scale neural networks. *Artificial life*, 15(2):185–212, 2009.
- [35] Kenneth O Stanley. Compositional pattern producing networks: A novel abstraction of development. *Genetic programming and evolvable machines*, 8(2):131–162, 2007.
- [36] Theofanis Karaletsos, Peter Dayan, and Zoubin Ghahramani. Probabilistic meta-representations of neural networks. *arXiv preprint arXiv:1810.00555*, 2018.
- [37] Theofanis Karaletsos and Thang D. Bui. Hierarchical gaussian process priors for bayesian neural network weights. In Hugo Larochelle, Marc’Aurelio Ranzato, Raia Hadsell, Maria-Florina Balcan, and Hsuan-Tien Lin, editors, *Advances in Neural Information Processing Systems (NeurIPS)*, 2020.

- [38] Charles D Gilbert and Mariano Sigman. Brain states: top-down influences in sensory processing. *Neuron*, 54(5):677–696, 2007.
- [39] JM Hupé, AC James, BR Payne, SG Lomber, P Girard, and J Bullier. Cortical feedback improves discrimination between figure and background by v1, v2 and v3 neurons. *Nature*, 394(6695):784–787, 1998.
- [40] Dean Wyatte, Tim Curran, and Randall O’Reilly. The limits of feedforward vision: Recurrent processing promotes robust object recognition when objects are degraded. *Journal of Cognitive Neuroscience*, 24(11):2248–2261, 2012.
- [41] Kaiming He, Xiangyu Zhang, Shaoqing Ren, and Jian Sun. Deep residual learning for image recognition. In *Proceedings of the IEEE conference on computer vision and pattern recognition*, pages 770–778, 2016.
- [42] Christian Szegedy, Wei Liu, Yangqing Jia, Pierre Sermanet, Scott Reed, Dragomir Anguelov, Dumitru Erhan, Vincent Vanhoucke, and Andrew Rabinovich. Going deeper with convolutions. In *Proceedings of the IEEE conference on computer vision and pattern recognition*, pages 1–9, 2015.
- [43] Rupesh Kumar Srivastava, Klaus Greff, and Jürgen Schmidhuber. Highway networks. *arXiv preprint arXiv:1505.00387*, 2015.
- [44] Varun Ramakrishna, Daniel Munoz, Martial Hebert, James Andrew Bagnell, and Yaser Sheikh. Pose machines: Articulated pose estimation via inference machines. In *European Conference on Computer Vision*, pages 33–47. Springer, 2014.
- [45] David H Wolpert. Stacked generalization. *Neural networks*, 5(2):241–259, 1992.
- [46] David Weiss and Benjamin Taskar. Structured prediction cascades. In *Proceedings of the Thirteenth International Conference on Artificial Intelligence and Statistics*, pages 916–923. JMLR Workshop and Conference Proceedings, 2010.
- [47] Xingjian Shi, Zhouong Chen, Hao Wang, Dit-Yan Yeung, Wai-Kin Wong, and Wang-chun Woo. Convolutional lstm network: A machine learning approach for precipitation nowcasting. *arXiv preprint arXiv:1506.04214*, 2015.
- [48] Andrej Karpathy and Li Fei-Fei. Deep visual-semantic alignments for generating image descriptions. In *Proceedings of the IEEE conference on computer vision and pattern recognition*, pages 3128–3137, 2015.
- [49] Volodymyr Mnih, Nicolas Heess, Alex Graves, and Koray Kavukcuoglu. Recurrent models of visual attention. In *Advances in Neural Information Processing Systems*, 2014.
- [50] Nicholas J Butko and Javier R Movellan. Optimal scanning for faster object detection. In *2009 IEEE Conference on Computer Vision and Pattern Recognition*, pages 2751–2758. IEEE, 2009.
- [51] Joao Carreira, Pulkit Agrawal, Katerina Fragkiadaki, and Jitendra Malik. Human pose estimation with iterative error feedback. In *Proceedings of the IEEE conference on computer vision and pattern recognition*, pages 4733–4742, 2016.
- [52] Ke Li, Bharath Hariharan, and Jitendra Malik. Iterative instance segmentation. In *Proceedings of the IEEE conference on computer vision and pattern recognition*, pages 3659–3667, 2016.
- [53] Amir R Zamir, Te-Lin Wu, Lin Sun, William B Shen, Bertram E Shi, Jitendra Malik, and Silvio Savarese. Feedback networks. In *Proceedings of the IEEE conference on computer vision and pattern recognition*, pages 1308–1317, 2017.
- [54] Yann LeCun, D Touresky, G Hinton, and T Sejnowski. A theoretical framework for back-propagation. In *Proceedings of the 1988 connectionist models summer school*, volume 1, pages 21–28, 1988.
- [55] Tiancai Wang, Xiangyu Zhang, and Jian Sun. Implicit feature pyramid network for object detection. *arXiv preprint arXiv:2012.13563*, 2020.
- [56] Samy Wu Fung, Howard Heaton, Qiuwei Li, Daniel McKenzie, Stanley Osher, and Wotao Yin. Fixed point networks: Implicit depth models with jacobian-free backprop. *arXiv preprint arXiv:2103.12803*, 2021.
- [57] Mykhaylo Andriluka, Leonid Pishchulin, Peter Gehler, and Bernt Schiele. 2d human pose estimation: New benchmark and state of the art analysis. In *Proceedings of the IEEE Conference on Computer Vision and Pattern Recognition*, pages 3686–3693, 2014.

- [58] Iro Armeni, Sasha Sax, Amir R Zamir, and Silvio Savarese. Joint 2d-3d-semantic data for indoor scene understanding. *arXiv preprint arXiv:1702.01105*, 2017.
- [59] Alejandro Newell, Kaiyu Yang, and Jia Deng. Stacked hourglass networks for human pose estimation. In *European conference on computer vision*, pages 483–499. Springer, 2016.
- [60] Wenxiao Wang, Cong Fu, Jishun Guo, Deng Cai, and Xiaofei He. Cop: Customized deep model compression via regularized correlation-based filter-level pruning. In *International Joint Conference on Artificial Intelligence*, 2019.
- [61] Andrei Barbu, David Mayo, Julian Alverio, William Luo, Christopher Wang, Dan Gutfreund, Josh Tenenbaum, and Boris Katz. Objectnet: A large-scale bias-controlled dataset for pushing the limits of object recognition models. *Advances in neural information processing systems*, 32:9453–9463, 2019.
- [62] Yang He, Ping Liu, Ziwei Wang, Zhilan Hu, and Yi Yang. Filter pruning via geometric median for deep convolutional neural networks acceleration. In *Proceedings of the IEEE/CVF Conference on Computer Vision and Pattern Recognition*, pages 4340–4349, 2019.
- [63] Yang He, Guoliang Kang, Xuanyi Dong, Yanwei Fu, and Yi Yang. Soft filter pruning for accelerating deep convolutional neural networks. In *Proceedings of the 27th International Joint Conference on Artificial Intelligence*, pages 2234–2240, 2018.
- [64] Xuanyi Dong, Junshi Huang, Yi Yang, and Shuicheng Yan. More is less: A more complicated network with less inference complexity. In *Proceedings of the IEEE Conference on Computer Vision and Pattern Recognition*, pages 5840–5848, 2017.

Appendices

A Pruning RPG Networks for Lower Inference Time

Can networks with recurrent parameter generators be pruned, so the inference time can be further reduced? As discussed in Section 5.5 of the main paper, there is room for RPG networks to be further pruned. We prune 30% backbone parameters by dropping weights with lowest ℓ_1 norm for ResNet18-RPG and ResNet34-RPG. Number of backbone parameters are 11M and 5.6M, respectively (Table 7). With 50% number of parameters and 70% FLOPs, the ImageNet top-1 accuracy only drops 1.2% and 0.9% for ResNet18 and ResNet34, respectively. This indicates RPG networks can be pruned to further reduce the inference time.

Table 7: Pruning ResNet-RPG on ImageNet. Pruned RPG networks have 50% number of parameters and 70% FLOPs as the plain ResNet. ResNet18-RPG and ResNet34-RPG both only have 1% performance drop.

	Acc. before (%)	# Param ↓	# FLOPs ↓	Acc. After (%)
Res18-RPG	70.2	50%	30%	69.0 (-1.2)
Res34-RPG	73.4	50%	30%	72.5 (-0.9)

B Proof to the Orthogonal Proposition

We provide proofs to the orthogonal proposition mentioned in Section 3 of the main paper. Suppose we have two vectors $\mathbf{f}_i = \mathbf{A}_i \mathbf{f}$, $\mathbf{f}_j = \mathbf{A}_j \mathbf{f}$, where $\mathbf{A}_i, \mathbf{A}_j$ are sampled from the $O(M)$ Haar distribution.

Proposition 1. $E [\langle \mathbf{f}_i, \mathbf{f}_j \rangle] = 0$.

Proof.

$$\begin{aligned}
\mathbb{E} [\langle \mathbf{f}_i, \mathbf{f}_j \rangle] &= \mathbb{E} [\langle \mathbf{f}_i, \mathbf{f}_j \rangle] \\
&= \mathbb{E} [\langle \mathbf{A}_i \mathbf{f}, \mathbf{A}_j \mathbf{f} \rangle] \\
&= \mathbb{E} [\langle \mathbf{f}, \mathbf{A}_i^T \mathbf{A}_j \mathbf{f} \rangle] \\
&= \mathbf{f}^T \mathbb{E} [\mathbf{A}_i^T \mathbf{A}_j] \mathbf{f} \\
&= 0
\end{aligned}$$

where $\mathbf{A}_i^T \mathbf{A}_j$ is equivalently a random sample from $O(M)$ Haar distribution and its expectation is clearly 0. \square

Proposition 2. $\mathbb{E} \left[\left\langle \frac{\mathbf{f}_i}{\|\mathbf{f}_i\|}, \frac{\mathbf{f}_j}{\|\mathbf{f}_j\|} \right\rangle^2 \right] = \frac{1}{M}$.

Proof.

$$\begin{aligned}
\mathbb{E} \left[\left\langle \frac{\mathbf{f}_i}{\|\mathbf{f}_i\|}, \frac{\mathbf{f}_j}{\|\mathbf{f}_j\|} \right\rangle^2 \right] &= \frac{\mathbb{E} [\langle \mathbf{A}_i \mathbf{f}, \mathbf{A}_j \mathbf{f} \rangle^2]}{\|\mathbf{f}\|_2^2 \|\mathbf{f}\|_2^2} \\
&= \mathbb{E} \left[\left\langle \mathbf{A} \frac{\mathbf{f}}{\|\mathbf{f}\|}, \frac{\mathbf{f}}{\|\mathbf{f}\|} \right\rangle^2 \right], \text{ where } \mathbf{A} = \mathbf{A}_i^T \mathbf{A}_j \sim O(M) \text{ Haar distribution}
\end{aligned}$$

Due to the symmetry,

$$= \mathbb{E} \left[\left\langle \mathbf{A} \frac{\mathbf{f}}{\|\mathbf{f}\|}, (1, 0, 0, \dots, 0)^T \right\rangle^2 \right]$$

Let $\mathbf{g} = \mathbf{A} \frac{\mathbf{f}}{\|\mathbf{f}\|}$,

$$\begin{aligned}
&= \mathbb{E} [g_1^2] \\
&= \frac{1}{M}
\end{aligned}$$

since \mathbf{g} is a random unit vector and $\mathbb{E} \left[\sum_{k=1}^M g_k^2 \right] = \sum_{k=1}^M \mathbb{E} [g_k^2] = 1$. \square